A DNN surrogate unsteady aerodynamic model for wind turbine loads calculations

Shreyas Ananthan[1], Ganesh Vijayakumar[1], Shashank Yellapantula[1]
[1]National Renewable Energy Laboratory, Golden Colorado, USA.
E-mail: shreyas.ananthan@nrel.gov

Abstract. A recurrent deep-neural network (DNN) surrogate model capable of modeling the unsteady aerodynamic response and dynamic stall behavior of wind turbine blades has been developed and validated for use in engineering design codes. The model is trained using a subset of the oscillating airfoil experiments conducted at the Ohio State University wind tunnel. The predictions from our DNN model show excellent agreement with the measured data and, in all cases, a marked improvement over the state-of-the-art unsteady aerodynamic models. The DNN-based unsteady aerodynamics model was integrated with OpenFAST to perform full-turbine load computations for the NREL-5MW rotor. The largest differences are observed for the inboard stations, particularly in the pitching moment response, when using the new surrogate model compared to the other models available in OpenFAST.

1. Introduction

Unsteady aerodynamic response of wind-turbine blades under turbulent inflow conditions is the primary driver of the fatigue loads experienced by wind turbine rotors. For large offshore rotors, these unsteady effects become more pronounced as the blades operate in regions of high shear, and sometimes negative shear in the presence of low-level jets. When combined with yaw-based controls strategy for wake steering, newer turbines will increasingly have to trade-off increased power output at farm level with fatigue load impacts on individual turbines. Accurate prediction of the unsteady aero-structural dynamic response, and the resulting fatigue loads, is crucial for robust design of the next-generation turbines. The models used in engineering design and optimization workflows must be capable of properly modeling the aerodynamic lag and hysterisis effects and the dynamic stall phenomena under a wide range of inflow conditions and Reynolds numbers across the blade.

While high-fidelity computational fluid dynamics (CFD) analyses [1, 2, 3] have shown great promise in resolving the flow features and predicting the unsteady aerodynamic loading, the computational overhead of CFD models make their choice impractical in routine load calculations within the blade design and optimization workflows. Current state-of-the-art engineering loads analysis codes employ reduced-order models that attempt to capture the key physics at an affordable computational cost. The most popular models used in wind-turbine applications are variants of either the Beddoes-Leishman (BL) [4, 5] or the Øye [6] models. These models introduce unsteady aerodynamic effects as a correction to the two-dimensional (2D) steady-state polars based on coefficients that are tuned using a limited set of parameters for specific applications using experimental datasets. For example, the Beddoes-Leishman model, originally

developed for helicopter applications operating in compressible regime, was tuned for thin, symmetric NACA0012 airfoil. Since then, several researchers have proposed modifications to the original BL model to make it suitable for wind-energy applications – predicting unsteady aerodynamic response for thick, cambered airfoil sections operating at low Mach numbers [7, 8]. One disadvantage of these models is that the empiricially tuned coefficients are a function of the airfoil geometry and must be tuned for different airfoils and Reynolds numbers. However, due to the limited number of tunable parameters available, the model might not perform as desired for the range of operating conditions of interest in wind turbine design.

The recent advances in machine learning techniques [9] offer an attractive alternative. These models can be trained using both experimental and CFD generated datasets to learn the unsteady aerodynamic response as a function of unsteady inflow conditions as well as the airfoil and blade geometry. Depending on the deep neural network (DNN) architecture employed by the surrogate machine learning model, they can be trained to capture the important aerodynamic effects for a wide range of airfoil families. The training process for the DNN surrogate models can be easily automated and repeated with very little effort with the availability of new datasets. Thus, these models can be continually improved as the blade design evolves.

This paper will document the fundamental methodology used to design and develop a new DNN surrogate model that can model the unsteady aerodynamic response. The performance of the trained surrogate model will be compared against the state-of-the-art unsteady aerodynamic models used in design codes today: Hansen et al. [7], Beddoes-Leishman [4, 5], and Øye [6]. Finally, the trained model will be integrated within OpenFAST [11], a comprehensive wind turbine analysis code, and used to study the turbine performance and loading under unsteady inflow conditions for the NREL-5MW rotor.

2. Methodology

We first provide a brief discussion of the key physics involved in unsteady aerodynamics response of wind turbines. The physics drivers will provide the rationale for the choice of the type of neural network model used in the current study as well as the choice of the inputs and outputs and the training process adopted in the development of the model. This will be followed by a description of the actual training process and the hyperparmeter optimization methodology.

2.1. Unsteady Aerodynamic Response and Dynamic Stall

In wind turbine applications, airfoil sections of a rotor blade experience temporal changes in angle of attack α due to various factors, including but not limited to unsteady turbulent inflow conditions, variations due to atmospheric boundary layer shear from blade rotation, pitch and blade torsional changes, etc. The airfoil polars (lift, drag, and pitching moment) don't respond instantaneously to the temporal variations in angle of attack but, instead, exhibit a characteristic *aerodynamic lag* that is a function of the reduced frequency κ ($= \omega c/2V_r$, where ω is the angular frequency of the variation in angle attack, c is the sectional chord length, and V_r is the local freestream velocity). The aerodynamic lag is usually observed as a *hysterisis loop* in the lift response when plotted as a function of angle of attack.

When the mean angle of attack is high enough, the airfoil exhibits the dynamic stall phenomenon that has four distinct stages – see Fig. 3. During the upstroke, as the angle of attack increases past the static stall angle of attack, a separation vortex forms near the leading-edge of the airfoil and begins convecting over the suction side of the airfoil. The fore-aft movement of the vortex leads to pitching moment stall, while the lift continues to increase. Eventually the vortex moves past the trailing edge of the airfoil and this leads to a dramatic drop in the lift coefficient (lift stall). Depending on the reduced frequency, the lift and pitching moment recovery often does not happen until the instantaneous angle of attack drops to values much lower than the static stall angle of attack. For aeroelastically tailored blades, dynamic stall

can induce a torsional response (through changes in the pitching moment) leading to complex aero-structural interactions. For further details the reader is referred to chapters 8 and 9 of Ref. [10].

2.2. DNN Surrogate for Unsteady Aerodynamics

Based on the description of the unsteady aerodynamics above, it is clear that any unsteady model developed would need to be capable of remembering the history the aerodynamic reponse to be able to accurately predict the instantaneous values of aerodynamic quantities of interest. Recurrent neural networks (RNN) are a class of machine learning algorithms that are particularly suited for dealing with temporal datasets [9, 12]. In particular, we choose a network architecture comprising of one or more series of long short-term memory (LSTM) [13] networks – see Fig. 1. LSTMs are attractive for the unsteady aerodynamics problem as they can handle long-term dependencies and are well-suited for making predictions based on time series data, i.e., temporal variation of angle of attack and freestream velocity. For a detailed discussion of LSTM cell and how it works, the reader is referred to Goodfellow et al. [12]. The present work uses Pytorch [14], an open-source Python library, to develop and train the DNN surrogate.

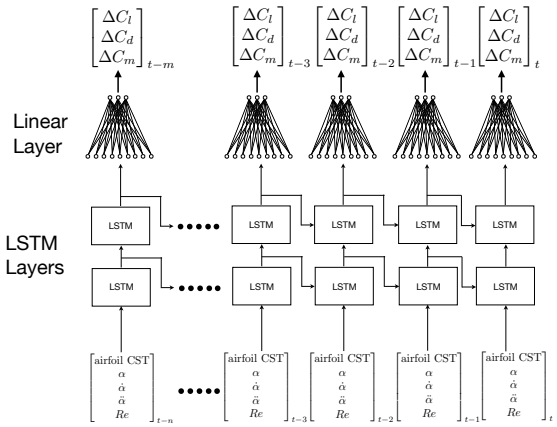

Figure 1. Schematic of the neural network used for the unsteady aerodynamics model.

2.2.1. Design of the DNN Surrogate Model The next step in the design of the surrogate model is choosing appropriate inputs and outputs for the model. As a starting point, we consider the inputs provided to the reduced-order models in use today: time-history of angle of attack, reduced frequency κ, and Reynolds number. While angle of attack and Reynolds number are easily computed for a turbine calculation, estimating a single reduced frequency to be used as input under unsteady turbulent inflow is not easy. Instead, we provide the first and second time derivatives of the angle of attack (computed using second-order backward differencing) as inputs instead of the reduced frequency. In engineering calculations, the aerodynamic performance is computed using airfoil lookup tables at a limited number of locations along the blade span and interpolated across the blade. To allow the surrogate model to capture the effects of changes in airfoil shape and thickness across the blade span, we provide airfoil geometry as inputs to the model in addition to the aerodynamic quantities discussed above. The airfoil geometry is parameterized with a universal parametric representation [15] that was developed at Boeing to specifically represent aerodynamic shapes with a few parameters. In the present work, the upper and lower surfaces of airfoil sections are parametrized with eighth-order Bernstein polynomials, allowing the entire geometry to be represented with just 18 coefficients.

The surrogate model is trained to capture the difference between the instantaneous lift, drag, and pitching moment values from the quasi-steady values in airfoil lookup tables. Training the model on the deltas instead of the absolute instantaneous value removes the sensitivity of the model to airfoil quasi-static behavior and makes it more applicable across a wider range of airfoil shapes.

Table 1. Candidate model parameters and hyperparameters

Model	LSTM cells	Hidden nodes per cell	Learning rate	Batch size	Total parameters
1	3	26	0.0014	4	16513
2	4	33	0.0014	8	34554
3	2	31	0.0017	4	14852

2.2.2. Training the DNN Surrogate The present work follows the training procedure described in Ref. [16], the surrogate model is trained on the dataset from Ohio State University wind tunnel tests provided by the National Wind Technology Center Information Portal [17]. The dataset contains comprehensive data on both static and dynamic lift, drag, and pitching moment characteristics for the 10 different airfoils – 9 airfoils of the S8XX family and the N4415 airfoil for a range of reduced frequencies as well as different mean angle of attack and amplitudes [18, 19]. The raw data contains experimental errors, high frequency fluctuations in aerodynamic loads, and large cycle-to-cycle variations in the aerodynamic response that are expected to present challenges in the development of the surrogate model.

The dataset contains over 1400 data points for 10 different airfoils with reduced frequencies ranging from $0.02 \leq \kappa \leq 0.1$, Reynolds numbers ranging from $0.75 - 1.5 \times 10^6$, mean angle of attack $\alpha_0 = 0°,\ 8°,$ and $14°$, and amplitude $\alpha_1 = 5°, 10°$. In the present analysis, we restrict our training data to turbulent cases only. This is due to the fact that turbulent transition characteristics are quite different between laminar and turbulent cases and there is not enough data to train the model to capture the transition. The dataset was partitioned into training and validation batches based on the reduced frequency. Datasets with reduced frequencies $0.03 \leq \kappa \leq 0.045$ were chosen to belong in the validation data and the remaining data was used as training data. This partitioning approach resulted in a roughly $80\% - 20\%$ between training and validation datasets.

2.2.3. Hyperparameter Optimization using SHERPA In our previous work [16], the DNN surrogate model was set up with two stacked LSTM layers, each with 64 hidden nodes, with fully connected layer that provided the outputs of the model. However, the choice of the number of LSTM cells, the hidden nodes, etc. was arbitrary and was not the optimal choice for the surrogate model in terms of its accuracy and computational efficiency. To rectify this deficiency, a hyperparameter optimization was performed using SHERPA [20], a python library for tuning machine learning models. In the current study, population based training (PBT) technique is used within SHERPA to optimize the number of LSTM layers, number of hidden nodes, batch size and learning rate of the stochastic gradient computation. PBT is a evolutionary algorithm that provides an optimization technique for finding the best combination of model parameters and training hyperparameters. The predicted mean square error (MSE) in the validation data is used as the metric to optimize hyperparameters. In addition to accuracy, computational efficiency (i.e., fewer number of parameters in the neural network) was also used as a criteria in choosing a final network amongst multiple candidates with similar MSE. Table 1 shows the final three candidates from SHERPA parameter search. Based on this analysis Model 3 was chosen for all subsequent studies.

3. Results

3.1. Hyperparameter Optimization Using SHERPA

One major improvement from the model in Ref. [16] is the use of SHERPA to determine an optimal network configuration. Four hyperparameters were chosen for the current study: 1. the number of LSTM cells in the surrogate model, 2. the number of hidden nodes within each

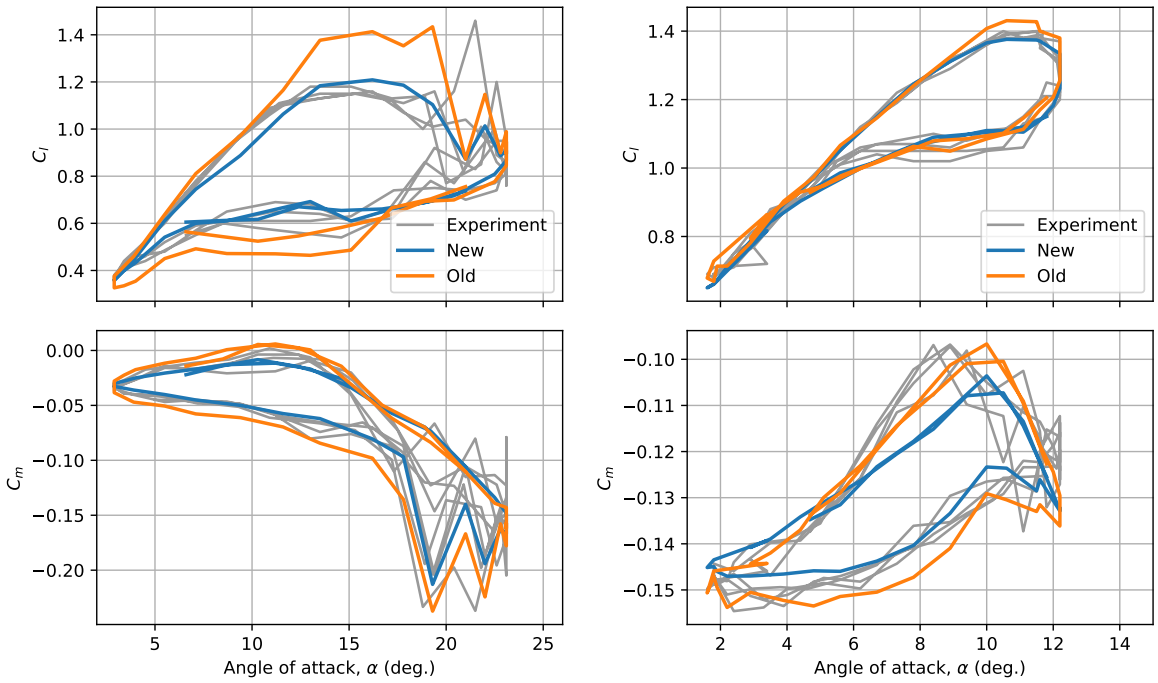

(a) S809; $\alpha_0 = 14°; \alpha_1 = 10°$ (b) S825; $\alpha_0 = 8°; \alpha_1 = 5°$

Figure 2. Comparison of the unsteady lift (C_l) and pitching moment (C_m) coefficient response to osciallatory angle of attack variations at different mean angle of attack (α_0) and amplitude (α_1) for the S809 and S825 airfoils. $Re = 1.25 \times 10^6, \kappa \approx 0.04$.

LSTM cell, 3. learning rate, and 4. the batch size. The training and validation phases used the dataset partitions that were described in Sec. 2.2.2 for each trial generated by SHERPA. A total of 300 epochs were used for each of the trials. Six generations with a population size of 20 were used to arrive at the optimal combination of hyperparameters: three LSTM cells with 26 hidden nodes within each cell, a batch size of four, and a learning rate of 0.0014. The hyperparameter optimization process was performed on a single NVIDIA Volta V100 GPU and took approximately six hours to complete. Based on the results of the SHERPA optimization process, the neural network configuration was updated from the original settings described in Ref. [16] to the following parameters. The training and validation process was also performed on a single NVIDIA Volta V100 GPU and takes approximately 6 minutes to complete.

Figure 2 shows the comparison of the original surrogate model from Ref. [16] and the new network architecture based on the optimized hyperparameters for the S809 and S825 airfoils. The new model shows much better agreement with the experimental measurements than the previous model. The new model does not overpredict the maximum lift and is observed to be better at capturing the reattachment point. Similar improvements are noted in the pitching moment hysteresis loop also. While only a subset of the validation data is shown in this paper, the model improvements are observed on all airfoils for all conditions considered.

In addition to a qualitative comparison of the improvements in Fig. 2, we also compute the L_2 norm error and compare the percent improvements for the two cases shown. The *improvement*

Table 2. Percent improvement in mean square error metric for the old [16] and new models for the S809 and S825 airfoils – see also Fig. 2. $Re = 1.25 \times 10^6, \kappa \approx 0.04$.

Case	I_{C_l}	I_{C_m}
S809; $\alpha_0 = 8°; \alpha_1 = 10°$	17.22	14.79
S825; $\alpha_0 = 8°; \alpha_1 = 5°$	33.12	-1.32

index I is computed using the mean squared error over the time duration as shown below

$$e = \sum_t (x_{\text{ML}} - x_{\text{expt}})^2 \qquad x = [C_l, C_m]$$

$$I_x = \left(1 - \frac{e_{\text{new}}}{e_{\text{old}}}\right) \times 100$$

Table 2 shows the improvements in the C_l and C_m predictions for the two cases shown in Fig. 2. Signficant improvements are observed for the predictions of the unsteady lift. For pitching moment, the S809 shows marked improvement but a slight increase in error for the S825 case.

3.2. Comparison With State-of-the-Art Unsteady Aerodynamics Models

The performance of the new DNN surrogate model is then compared to the state-of-the-art unsteady aerodynamics models used in engineering design codes: Beddoes-Leishman (BL) model [4], Hansen et al. [7], and Øye [6]. Figure 3 shows the non-dimensional, unsteady lift and pitching moment response as a function of angle of attack for the N4415, S809, S812, and S825 airfoils. All cases shown in the figure are operating at a Reynolds number $Re = 1.25 \times 10^6$ and a reduced frequency $\kappa \approx 0.04$. The mean angle of attack $\alpha_0 = 8°$ and the amplitude of angle of attack oscillation $\alpha_1 = 10°$. For these operating conditions, all four airfoils show the classic dynamic stall behavior discussed in Sec. 2.1. Unlike the DNN surrogate model results shown in Fig. 2, where the angle of attack time-history from experimental data was directly used as inputs to the DNN surrogate model, the results shown in Fig. 3 use the same sinusoidal signal that was provided to the other models.

All unsteady aerodynamics models considered capture the qualitative nature of the lift hysterisis loop. However, the DNN surrogate shows marked improvement over the other models in capturing the maximum lift and stall behavior during the upstroke, and the flow recovery and eventual reattachment behavior during the downstroke. In general, the empirical models tend to exaggerate the crossover behavior for angles of attack less than the mean value, this is not observed in the experimental data or the surrogate model. Significant improvements in pitching moment predictions are observed when using the DNN surrogate model compared to the empirical models. None of the engineering models capture the width of the hystersis loop in the pitching moment response observed in the experiment. Several models miss the mangitude of the nose down pitching moment at maximum angle of attack.

3.3. NREL-5MW Rotor Simulations

Following the successful validation of the DNN surrogate model for unsteady, two-dimensional airfoil performance, the model was integrated with OpenFAST [11] loads analysis code. Simulations were performed for the NREL-5MW [21] at two wind speeds – 8 and 13 m/s with turbulent inflow ($TI = 10\%$) generated using Turbsim. The ElastoDyn beam model was used for predicting the structural deformations and loads on the blade.

Figure 4 shows the performance predictions for the two windspeeds from OpenFAST simulations with the new DNN surrogate model, Beddoes-Leishman model, and quasi-steady aerodynamics only. The plots show sectional angle of attack, lift and pitching moment at two

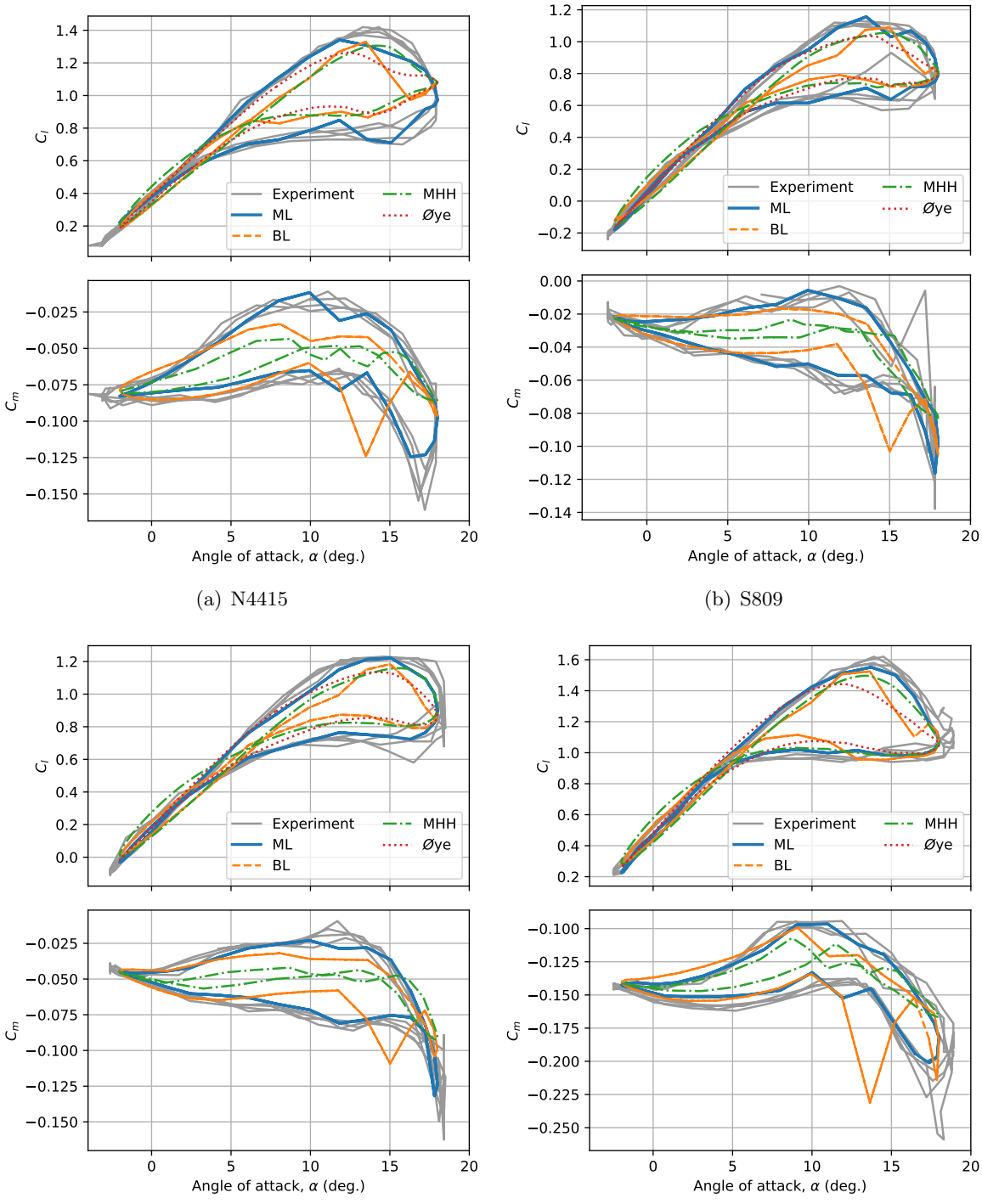

(a) N4415 (b) S809

(c) S812 (d) S825

Figure 3. Comparison of the DNN surrogate model predictions of unsteady lift (C_l) and pitching moment (C_m) response with popular models used in engineering codes and experimental data for the N4415, S809, S812, and S825 airfoils. $\alpha_0 = 8°; \alpha_1 = 10°; Re = 1.25 \times 10^6; \kappa \approx 0.04$. ML – DNN surrogate model; BL – Beddoes-Leishman model; MHH – Hansen et al. model; Øye – Øye dynamic stall model.

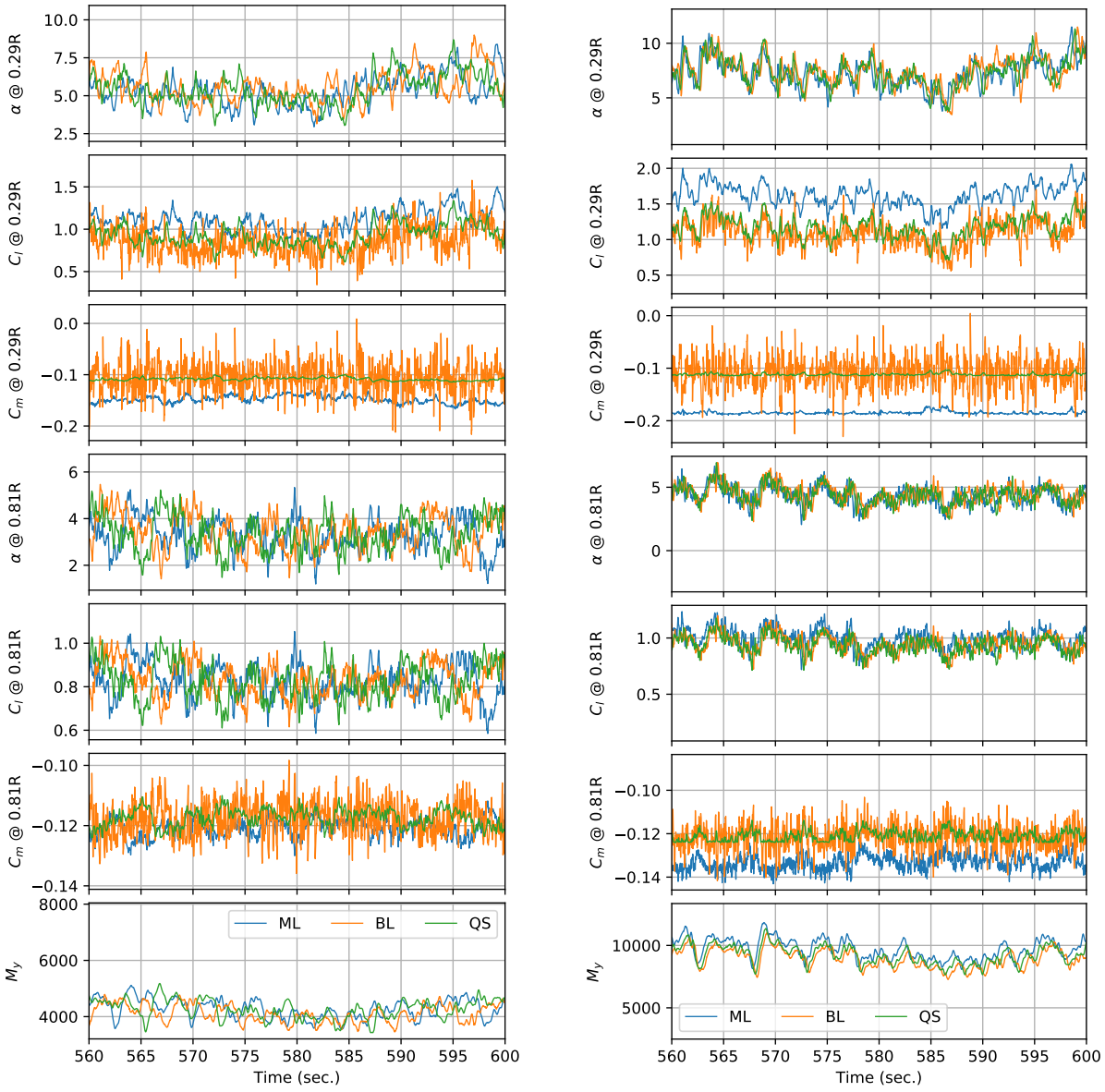

(a) $U_\infty = 8$ m/s (b) $U_\infty = 13$ m/s

Figure 4. Predictions of the sectional aerodynamic response and integrated root bending moment for NREL-5MW rotor operating at $U_\infty = 8$ and 13 m/s. $TI = 10\%$. ML – DNN surrogate model; BL – Beddoes-Leishman model; QS – Quasi-steady aerodynamics only.

radial stations, 30%R and 80%R for the reference blade, as well as the root bending moment for the last 100 seconds of a 600 second simulation. The outboard section is operating at a very low angle of attack and the lift and pitching moment response is very similar for this section for all three models considered. Larger differences are observed between the DNN surrogate predictions of the pitching moment than for the other two models in the inboard section. This difference is more pronounced for the 13 m/s case (region III) than for the 8 m/s case (region II). The differences in lift and pitching moment response for the 13 m/s case warrants further investigation. However, there are no significant differences observed in the root

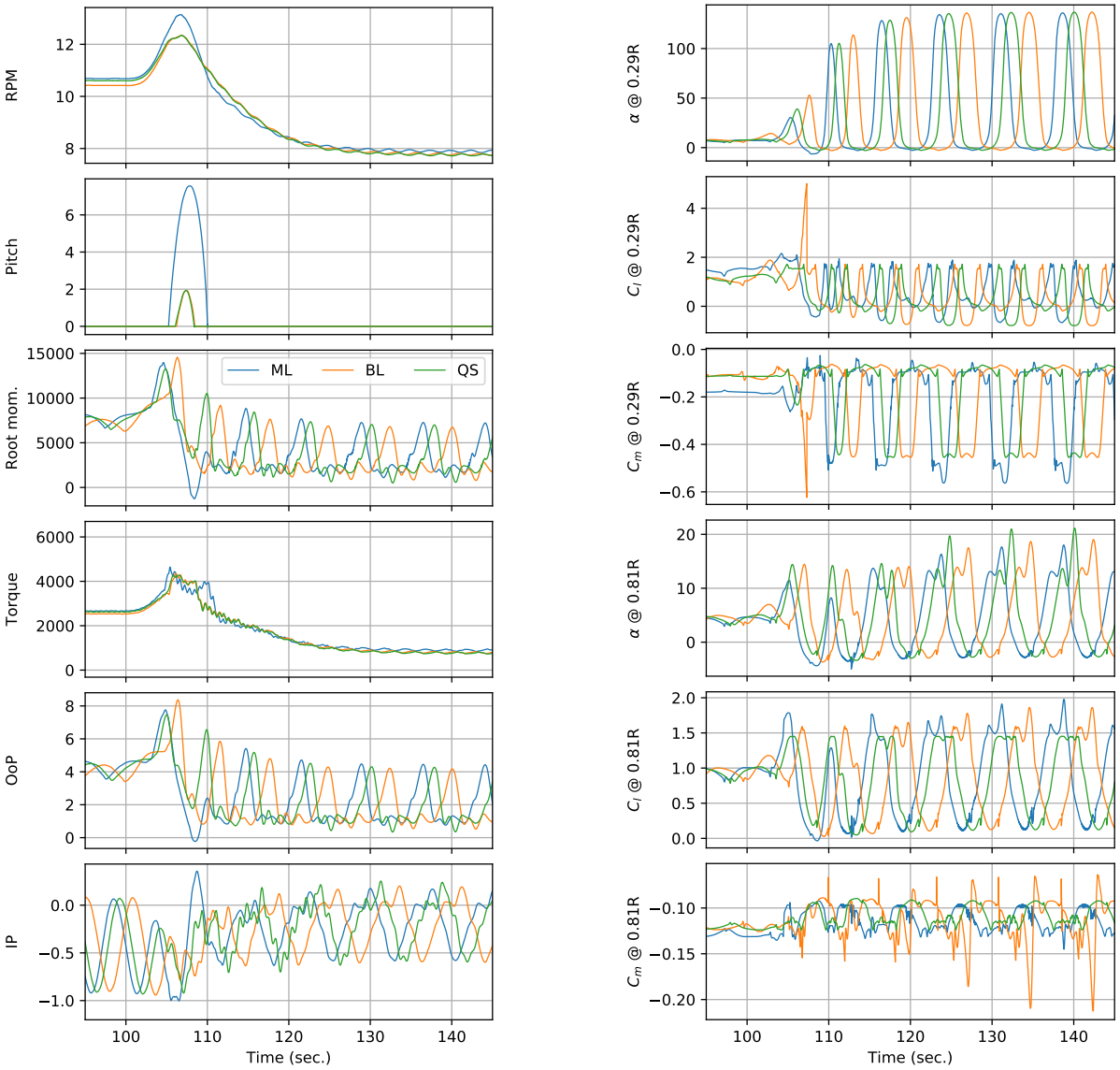

Figure 5. Performance predictions for the NREL-5MW rotor operating in a coherent gust, extreme change of direction condition (DLC 1.4). Left column: rotor RPM, blade pitch (deg.), root bending moment (Nm), rotor torque (Nm), out-of-plane, and in-plane tip deflections (m); right column: angle of attack, lift and pitching moment coefficients at 0.29R and 0.81R.

flapwise bending moment (M_y) response between the different models. These runs demonstrate successful integration of the DNN surrogate model with the OpenFAST code and the capability of the surrogate to behave as expected for airfoil sections that it was not trained on (DU and NACA63 series airfoils).

In order to evaluate the model performance in situations where the rotor blade has stalled we considered the coherent gust with extreme change of direction (EOD) (DLC 1.4) load case next. The turbine is operating in a uniform inflow with no turbulence at 9.4 m/s for the first 100 seconds. Over the next 10 seconds, the wind speed ramps up to 24.4 m/s and stays constant thereafter. During the same period, the wind direction changes from 0° to 76.6° and stays constant thereafter. Simulation is performed for a total duration of 200 seconds. Figure 5

shows the predicted performance time histories using the three different aerodynamic models in OpenFAST as described in the previous section. Compared to the previous case, larger differences are observed for the EOD case as the angles of attack increase past the static stall limit for almost all sections across the blade. The DNN surrogate model predicts much higher lift values between 100-110 seconds, followed by a steeper stall behavior compared to Beddoes-Leishman model. The stronger stall behavior is also evident in the root bending moment and out-of-plane deflection time histories. Past 110 seconds, the unsteady response is comparable between the three models, except for the phase differences between the three models.

4. Conclusions

A deep neural network surrogate model capable of predicting the unsteady aerodynamic response and dynamic stall behavior of wind-turbine rotors was developed. The DNN model consists of three stacked long short-term memory (LSTM) cells connected a linear layer. A hyperparameter optimization methodology was used to determine the optimal number of LSTM cells, the number of hidden nodes, the batch size, and learning rate during the training phase of the surrogate model. Hyperparameter optimization process was shown to have improved the model performance compared to the original model proposed in Ref. [16].

The trained model shows excellent agreement with measurements for different airfoils compared to the state-of-the-art empiricial models. The model was added as an alternative to the default Beddoes-Leishman model available in OpenFAST. Full turbine simulations were performed for the NREL-5MW rotor. Results demonstrate that the model behaves as expected for full turbine simulations even though the model was never trained for the airfoil sections or the inflow conditions for the NREL-5MW rotor. A coherent gust extreme change of direction case was also considered to examine the differences between the unsteady aerodynamics and stall behavior predicted by the DNN surrogate compared to the Beddoes-Leishman model. While differences are observed, the lack of validation data makes it difficult to asses the predictive capabilities of the new model.

While initial results are promising, the model has been trained on a limited data set and its efficacy at operational Reynolds numbers of modern wind turbines is still an open question and subject of ongoing research. Future work will attempt to enhance the model with additional datasets at conditions more relevant to modern wind turbines. Validation of the unsteady aerodynamics and the resulting loads predictions for full-turbine simulation will also be a focus of future studies.

5. Acknowledgements

The authors would like to acknowledge Dr. Emmanuel Branlard (NREL) for providing the results for the Hansen et al. and Øye models shown in Fig. 3. The authors would also like to acknowledge Dr. Evan Gaertner (NREL) for providing the OpenFAST simulation setup for DLC 1.4 – extreme change of direction (EOD) case analyzed in Fig. 5.

This work was authored by the National Renewable Energy Laboratory, operated by Alliance for Sustainable Energy, LLC, for the US Department of Energy (DOE) under Contract No. DE-AC36-08GO28308. Funding provided by the US Department of Energy Office of Energy Efficiency and Renewable Energy Wind Energy Technologies Office. A portion of this research was performed using computational resources sponsored by the Department of Energy's Office of Energy Efficiency and Renewable Energy and located at the National Renewable Energy Laboratory.

6. References

[1] Sørensen N N and Johansen J 2008 Upwind, aerodynamics and aero-elasticity, rotor aerodynamics in atmospheric shear flow *2007 European Wind Energy Conference and Exhibition* (Milan, Italy)

[2] Sørensen N N, Michelsen J A and Schreck S 2002 *Wind Energy* **5** 151–169
[3] Sprague M A, Ananthan S, Vijayakumar G and Robinson M 2019 Exawind: A multifidelity modeling and simulation environment for wind energy *NAWEA/WindTech 2019 Conference* (Amherst, MA)
[4] Leishman J G and Beddoes T S 1986 A generalized method for unsteady airfoil behavior and dynamic stall using indicial method *42nd Annual Forum of the American Helicopter Society* (Washington, D. C.)
[5] Leishman J G and Beddoes T S 1989 *Journal of the American Helicopter Society* **34** 3–17
[6] Øye S 1991 Dynamic stall simulated as time lag of separation *Proceedings of the 4th IEA Symposium on the Aerodynamics of Wind Turbines, Rome*
[7] Hansen M H, Gaunaa M and Aagaard Madsen H 2004 A Beddoes-Leishman type dynamic stall model in state-space and indicial formulations Tech. Rep. Risø-R-1354 (EN)
[8] Guntur S, Sørensen N N, Schreck S and Bergami L 2016 *Wind Energy* **19** 383–397
[9] LeCun Y, Bengio Y and Hinton G 2015 *Nature* **521**
[10] Leishman G J 2006 *Principles of Helicopter Aerodynamics* Cambridge Aerospace Series
[11] Jonkman J M 2013 The new modularization framework for the FAST wind turbine CAE tool *Proceedings of the 51st AIAA Aerospace Sciences Meeting including the New Horizons Forum and Aerospace Exposition* (Grapevine, Texas) URL https://www.nrel.gov/docs/fy13osti/57228.pdf
[12] Goodfellow I, Bengio Y and Courville A 2016 *Deep Learning* (MIT Press) chap Sequence Modeling: Recurrent and Recursive Nets http://www.deeplearningbook.org
[13] Hochreiter S and Schmidhuber J 1997 *Neural computation*
[14] Paszke A, Gross S, Massa F, Lerer A, Bradbury J, Chanan G, Killeen T, Lin Z, Gimelshein N, Antiga L, Desmaison A, Kopf A, Yang E, DeVito Z, Raison M, Tejani A, Chilamkurthy S, Steiner B, Fang L, Bai J and Chintala S 2019 Pytorch: An imperative style, high-performance deep learning library *Advances in Neural Information Processing Systems 32* ed Wallach H, Larochelle H, Beygelzimer A, d'Alché-Buc F, Fox E and Garnett R (Curran Associates, Inc.) pp 8024–8035 URL http://papers.neurips.cc/paper/9015-pytorch-an-imperative-style-high-performance-deep-learning-library.pdf
[15] Kulfan B M 2008 *Journal of Aircraft* 142–158
[16] Vijayakumar G, Yellapantuala S, Branlard E and Ananthan S 2019 Enhancement of unsteady and 3D aerodynamics models using machine learning *NAWEA/WindTech 2019 Conference* (Amherst, MA)
[17] NWTC Information Portal: OSU Wind-Tunnel Tests URL https://wind.nrel.gov/airfoils/OSU_data/
[18] Ramsay R R, Hoffmann M J and Gregorek G M 1995 Effects of Grit Roughness and Pitch Oscillations on the S809 Airfoil Tech. Rep. NREL/TP-442-7817 National Renewable Energy Laboratory
[19] Ramsay R R and Gregorek G M 1998 Effects of Grit Roughness and Pitch Oscillations on the S824 Airfoil Tech. rep. National Renewable Energy Laboratory
[20] Hertel L, Collado J, Sadowski P and Baldi P 2018 SHERPA: Hyperparameter optimization for machine learning models *32nd Conference on Neural Information Processing Systems (NIPS 2018)*
[21] Jonkman J, Butterfield S, Musial W and Scott G 2009 Definition of a 5-MW Reference Wind Turbine for Offshore System Development Tech. Rep. NREL/TP-500-38060 National Renewable Energy Laboratory